

Supplementary Information

Formation of Nanometer-Thick Water Layer at High Humidity on Dynamic Crystalline Material Composed of Multi-Interactive Molecules Revealed by Powder Structure Determination

Yumi Yakiyama, Gil Ryeong Lee, Sung Yeon Kim, Yoshitaka Matsushita, Yasushi Morita, Moon
Jeong Park and Masaki Kawano*

Contents:

Materials and Methods	S3
Sample preparation of K^+TPHAP^- crystalline powder 1	S3
Figure S1: Single crystal structures of K^+TPHAP^-	
Sample preparation of fully-hydrated K^+TPHAP^- powder 2	S5
Drying process of fully-hydrated K^+TPHAP^- powder 2	S5
X-ray powder structure analysis of 1-min dried K^+TPHAP^- powder	S5
Figure S2: XRPD analysis of 1 min-dried powder	
X-ray powder structure analysis of fully-hydrated K^+TPHAP^- powder 2	S7
Figure S3: Four possible structural answers of fully-hydrated K^+TPHAP^- powder 2	
X-ray powder structure analysis of 1-day dried K^+TPHAP^- powder 3	S10
Water adsorption measurement	S12

Table S1: Water adsorption result using pellet sample of K^+TPHAP^- crystalline powder 1

Determination of diffusion coefficient of water in 2 by PFG $^1\text{H-NMR}$	S12
Figure S4: The results of PFG $^1\text{H-NMR}$ of K^+TPHAP^- powders 1 and 2	
IR measurement of K^+TPHAP^- powders	S13
Figure S5: Blue shift of C=N and C=C stretching bands in IR spectra of K^+TPHAP^- by hydration	
Ionic conductivity measurement	S14
Figure S6: PXRD pattern change of pellet and non-pressed samples	
Figure S7: The pellet shapes of 1 before and after hydration	
Figure S8: Arrhenius plot of 1 at 95% RH	
Figure S9: Nyquist plot of K^+TPHAP^- at 95%RH, 25 °C	
References	S18

Materials and Methods

All chemicals were reagent grade and were used as received. All operations were performed at ambient temperature in air. IR spectra were recorded on a Varian 670-IR FT-IR spectrometer by the ATR method. All XRPD data for powder structure analyses except 1-day dried powder **3** were collected at PAL (Pohang Accelerator Laboratory). The XRPD data of **3** was collected on a Bruker D8 ADVANCE using CuK α radiation in house. The details are described below. Elemental analyses were performed at Pohang University of Science and Technology. Solid state and pulse field gradient (PFG) ^1H NMR measurements were performed on a Bruker DSX 400 MHz NMR system at KBSI Deagu Center, Korea.

Sample preparation of K^+TPHAP^- crystalline powder **1**

Single crystals of K^+TPHAP^- were prepared by the vapor diffusion method using MeOH solution of carefully purified K^+TPHAP^- and ethyl acetate.^{S1} Crystal structures are shown in fig. S1. A small amount of impurity (mainly KCl) can cause the significant degradation of the XRPD pattern after hydration. K^+TPHAP^- crystalline powder **1** was prepared by grinding the single crystals of K^+TPHAP^- with a pestle. Powder **1** was used for making pellets for further conductivity measurements (*vide infra*).

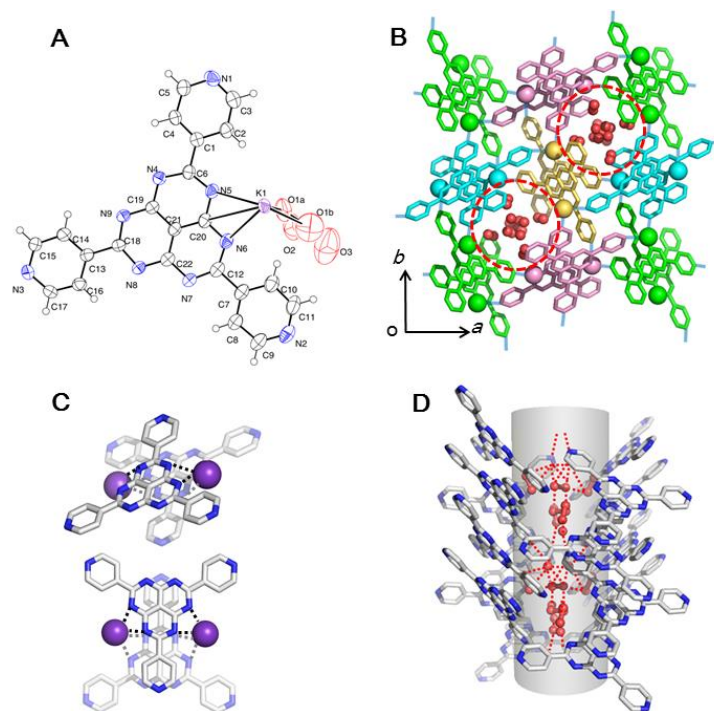


Figure S1. Single crystal structures of K^+TPHAP^- . **(A)** Thermal-ellipsoid diagram (50% probability level) of a molecular structure of K^+TPHAP^- . **(B)** Water encapsulating network structure composed of the dimer units of TPHAP^- s viewed from the c -axis. The dimer units are represented in pink, light green, light blue and yellow, respectively. The ionic bond between nitrogen atoms on pyridine and K^+ are shown by pale blue lines. Red dotted circles represent 1D water channels. Water molecules are shown as red spheres. **(C)** Top: Light blue dimer unit of K^+TPHAP^- in Figure S1A. Bottom: Overlap mode of the dimer unit. Face to face distance is 3.34 Å. Black dotted lines represent the ionic bonds between nitrogen atoms and K^+ . **(D)** 1D channel structure viewed from the b -axis. 1D channel is represented as a grey tube. Red dotted lines represent $\text{OH}\cdots\text{N}$ type hydrogen bonds between water and nitrogen atoms on the pyridine moiety. Except Figure S1A, each atom is represented as follows; C, grey; N, blue; O, red; K, purple. Hydrogen atoms are omitted for clarity.

Sample preparation of fully-hydrated K⁺TPHAP⁻ powder 2

Fully-hydrated powder **2** was prepared by keeping K⁺TPHAP⁻ single crystals at 95% RH and 25 °C for 1 day in a sealed plastic container. In order to keep the hydrated condition during XRPD measurements, we used a commercially available dorm type airtight cell (Bruker AXS) with additional water mist. Transfer of the sample from the hydration container to the airtight cell was performed as quickly as possible.

Drying process of fully-hydrated K⁺TPHAP⁻ powder 2

We observed the drying process of fully-hydrated powder **2** by keeping it for 20 sec at 20% RH, 20 °C and measuring its powder pattern with an air tight cell. This operation was repeated 3 times (total drying time: 1 min), then we kept the powder under the same condition to prepare 1-day dried powder **3**. Elemental analysis of 1-day dried powder **3** is as follows:

Calcd. (%) for C₂₂H₁₂N₉K(H₂O)_{5.1}: C, 49.54; H, 4.20; N, 23.63. Found: C, 49.31; H, 3.96; N, 23.52.

X-ray powder structure analysis of 1-min dried K⁺TPHAP⁻ powder

The XRPD pattern of 1-min dried K⁺TPHAP⁻ powder was recorded at 298 K in reflection mode [Bragg-Brentano geometry; synchrotron radiation $\lambda = 1.4639 \text{ \AA}$; 2θ range, 3.50 to 124.00°; step width, 0.01°; data collection time, 3 h 50 min] on a diffractometer equipped with multi-scintillation detectors at 9B HRPD beam line, PAL.

The XRPD pattern of 1-min dried powder was indexed with the program DICVOL91^{S2} to give an monoclinic cell ($a = 20.63897 \text{ \AA}$, $b = 15.98468 \text{ \AA}$, $c = 16.68509 \text{ \AA}$, $\beta = 100.029(3)^\circ$, $V = 5420.422 \text{ \AA}^3$) with good figures of merit. The space group was assigned from systematic absences as $P2/a$. Unit cell and profile refinement were carried out using the Pawley method, led to good fit ($R_{wp} = 17.79\%$, $\chi^2 = 17.338$) for these lattice parameters and space group. Structure solution was carried out by the simulated annealing method with the program DASH.^{S3} Models were input by using a constrained Z-matrix description and the molecular geometry of TPHAP⁻ was imported from the known crystal structure.^{S1} 30 runs of 3×10^7 Monte Carlo moves each were performed. The best structure obtained (Profile $\chi^2 = 6.36$) was taken as the starting structural model for Rietveld refinement. We attempted several numbers of water (3 to 10 molecules) and potassium ions (one atom with occ. = 1 or two atoms with occ. = 0.5) with one TPHAP as initial models. The best model for the structure determination was two potassium atoms with 0.5 occupancy factors, ten disordered water molecules, and two TPHAP with 0.5 occupancy factors. In the case of one TPHAP, we could not obtain acceptable molecular geometry, residual intensity and reasonable water positions with moderate peak intensities. Those are common features that we observed for severely disordered structures.

The Rietveld refinement was performed with the program RIETAN-FP^{S4} and VESTA.^{S5} Bond-angle restraints were employed to maintain the molecular geometry of TPHAP where the pyridyl rings were allowed to freely rotate. A uniform temperature factor was applied to all atoms as a constant.

Final Rietveld refinement result: $a = 20.656(6) \text{ \AA}$, $b = 15.978(4) \text{ \AA}$, $c = 16.80(1) \text{ \AA}$, $\beta = 100.68(3)^\circ$, $V = 5449(4) \text{ \AA}^3$, $R_{wp} = 5.575\%$ ($R_e = 8.674\%$), $R_p = 3.844\%$, $R_B = 0.455\%$, $R_F = 0.497\%$; 4151 profile points (2θ range, 3.5 to 45°); 227 refined variables. The structural information is shown in fig. S2.

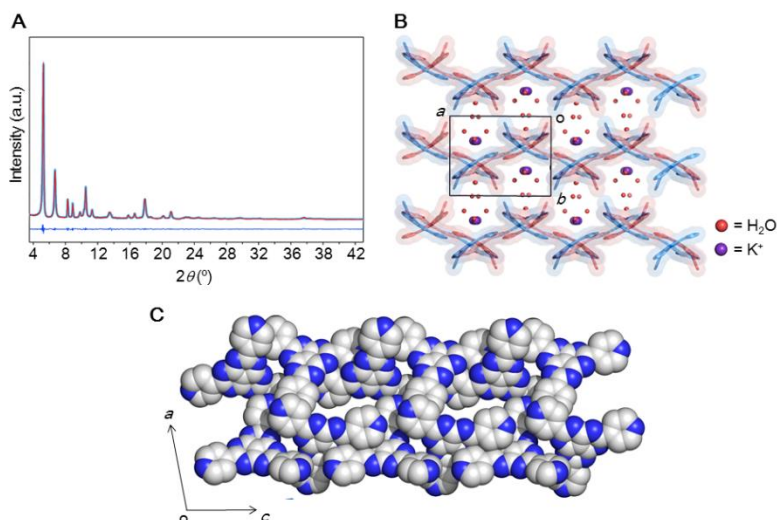


Figure S2. XRPD analysis of 1-min dried powder. **(A)** Experimental (red), calculated (pale blue), and difference (blue) of profiles obtained by the final Rietveld refinement of 1-min dried powder. Synchrotron X-ray radiation $\lambda = 1.4639 \text{ \AA}$. Cell parameter: $a = 20.656(6) \text{ \AA}$, $b = 15.979(4) \text{ \AA}$, $c = 16.80(1) \text{ \AA}$, $\beta = 100.68(3)^\circ$. **(B)** 1D channel structure of 1 min dried powder **3**. Both red and blue part show two disordered frameworks. **(C)** Staggered arrangement of TPHAP^- s along c axis. Color code: C, gray; N, blue; K, purple; O of H_2O , red.

X-ray powder structure analysis of fully-hydrated K^+TPHAP^- powder **2**

A XRPD pattern of fully-hydrated K^+TPHAP^- powder **2** was recorded at 298 K in reflection mode [Bragg-Brentano geometry; synchrotron radiation $\lambda = 1.46390 \text{ \AA}$; 2θ range, 3.00 to 123.50°; step width, 0.01°; data collection time, 9 h 30 min] on a diffractometer equipped with multi-scintillation detectors at 9B HRPD beam line, PAL.

The XRPD pattern of fully-hydrated powder **2** was indexed with the program DICVOL91^{S2} to give an monoclinic cell ($a = 24.09972 \text{ \AA}$, $b = 19.47807 \text{ \AA}$, $c = 16.65919 \text{ \AA}$, $\beta = 122.309^\circ$, $V = 6609.342 \text{ \AA}^3$) with

good figures of merit. The space group was assigned from systematic absences as $P2/n$. Unit cell and profile refinement were carried out using the Pawley method, led to good fit ($R_{wp} = 22.34\%$, $\chi^2 = 9.598$) for these lattice parameters and space group. Structure solution was carried out by the simulated annealing method with the program DASH.^{S3} Models were input by using a constrained Z-matrix description and the molecular geometry of TPHAP⁻ was imported from the known crystal structure.^{S1} 30 runs of 3×10^7 Monte Carlo moves each were performed. The best structure obtained (Profile $\chi^2 = 58.87$) was taken as the starting structural model for Rietveld refinement. We attempted several numbers of water (5 to 12 molecules) and potassium ions (one atom with occ. = 1 or two atoms with occ. = 0.5) as initial models. Because technically it was impossible to distinguish disordered water and potassium ions, we proposed four possible answers (type A-D) (fig. S3). The best model for the structure determination was type C: two potassium atoms with 0.5 occupancy factors and 8.5 disordered water molecules with one TPHAP.

The Rietveld refinement was performed with the program RIETAN-FP^{S4} and VESTA.^{S5} Bond-angle restraints were employed to maintain the molecular geometry of TPHAP where the pyridyl rings were allowed to freely rotate. A uniform temperature factor was applied to all atoms as a constant.

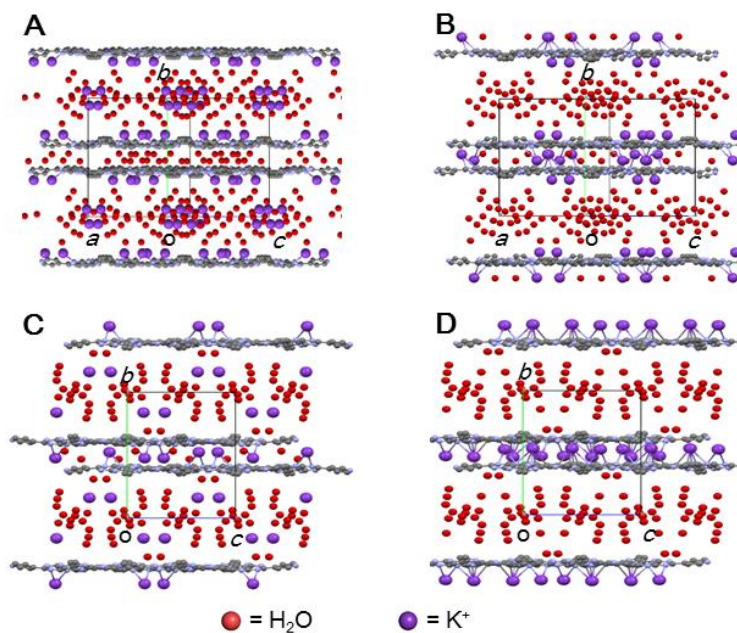


Figure S3. Four possible structural answers of fully-hydrated K^+TPHAP^- powder **2**. Final Rietveld refinement result for type A: $a = 24.126(5) \text{ \AA}$, $b = 19.459(2) \text{ \AA}$, $c = 16.672(4) \text{ \AA}$, $\beta = 122.49(1)^\circ$, $V = 6602(3) \text{ \AA}^3$, $R_{\text{wp}} = 10.719\%$ ($R_e = 10.688\%$), $R_p = 7.217\%$, $R_B = 6.690\%$, $R_F = 10.822\%$; 4645 profile points (2θ range, 3 to 49.44°); 217 refined variables. Final Rietveld refinement result for type B: $a = 24.121(6) \text{ \AA}$, $b = 19.458(2) \text{ \AA}$, $c = 16.668(5) \text{ \AA}$, $\beta = 122.48(2)^\circ$, $V = 6600(3) \text{ \AA}^3$, $R_{\text{wp}} = 10.759\%$ ($R_e = 10.682\%$), $R_p = 7.366\%$, $R_B = 7.039\%$, $R_F = 9.573\%$; 4645 profile points (2θ range, 3 to 49.44°); 222 refined variables. Final Rietveld refinement result for type C: $a = 24.131(5) \text{ \AA}$, $b = 19.458(2) \text{ \AA}$, $c = 16.672(4) \text{ \AA}$, $\beta = 122.52(2)^\circ$, $V = 6601(3) \text{ \AA}^3$, $R_{\text{wp}} = 10.700\%$ ($R_e = 10.689\%$), $R_p = 7.145\%$, $R_B = 6.738\%$, $R_F = 10.349\%$; 4645 profile points (2θ range, 3 to 49.44°); 216 refined variables. Final Rietveld refinement result for type D: $a = 24.120(4) \text{ \AA}$, $b = 19.455(3) \text{ \AA}$, $c = 16.659(3) \text{ \AA}$, $\beta = 122.48(1)^\circ$, $V = 6595(2) \text{ \AA}^3$, $R_{\text{wp}} = 10.804\%$ ($R_e = 10.689\%$), $R_p = 7.231\%$, $R_B = 7.367\%$, $R_F = 11.733\%$; 4645 profile points (2θ range, 3 to 49.44°); 216 refined variables.

X-ray powder structure analysis of 1-day dried K⁺TPHAP⁻ powder 3

A XRPD pattern of 1-day dried K⁺TPHAP⁻ powder 3 was recorded at 298 K in reflection mode [Bragg-Brentano geometry; X-ray radiation $\lambda = 1.5406 \text{ \AA}$; 2θ range, 3.00 to 50.00°; step width, 0.0184°; data collection time, 3 h] on a Bruker D8 ADVANCE using CuK α radiation in house.

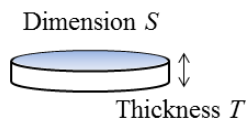
The XRPD pattern of 1-day dried K⁺TPHAP⁻ powder 3 was indexed with the program DICVOL91^{S2} to give an monoclinic cell ($a = 20.92036 \text{ \AA}$, $b = 15.94678 \text{ \AA}$, $c = 9.75110 \text{ \AA}$, $\beta = 104.663^\circ$, $V = 3147.142 \text{ \AA}^3$) with good figures of merit. The space group was assigned from systematic absences as $P2/a$. Unit cell and profile refinement were carried out using the Pawley method, led to good fit ($R_{wp} = 10.08\%$, $\chi^2 = 3.198$) for these lattice parameters and space group. Structure solution was carried out by the simulated annealing method with the program DASH.^{S3} Models were input by using a constrained Z-matrix description and the molecular geometry of TPHAP⁻ was imported from the known crystal structure.^{S1} 30 runs of 3×10^7 Monte Carlo moves each were performed. The best structure obtained (Profile $\chi^2 = 15.61$) was taken as the starting structural model for Rietveld refinement. We attempted several numbers of water (2 to 6 molecules) and potassium ions (one atom with occ. = 1 or two atoms with occ. = 0.5) as initial models. The best model for the structure determination was obtained with one potassium atom with 1.0 occupancy factors and two ordered water molecules.

The Rietveld refinement was performed with the program RIETAN-FP^{S4} and VESTA.^{S5} Bond-angle restraints were employed to maintain the molecular geometry of TPHAP where the pyridyl rings were allowed to freely rotate. A uniform temperature factor was applied to all atoms as a constant.

Final Rietveld refinement result: $a = 20.90(1) \text{ \AA}$, $b = 15.93(1) \text{ \AA}$, $c = 9.711(5) \text{ \AA}$, $\beta = 104.65(3)^\circ$, $V = 3128(3) \text{ \AA}^3$, $R_{wp} = 4.847\%$ ($R_e = 7.351\%$), $R_p = 3.043\%$, $R_B = 1.002\%$, $R_F = 0.953\%$; 2498 profile points (2θ range, 3 to 49.44°); 185 refined variables.

CCDC 952977 (water exchanged K^+TPHAP^- single crystal), 1031002 (1-day dried K^+TPHAP^- powder, **3**), 1031003 (1-min dried K^+TPHAP^- powder) and 1031004 (fully-hydrated K^+TPHAP^- powder, **2**, type C) contains the supplementary crystallographic data for this paper. These data can be obtained free of charge from The Cambridge Crystallographic Data Centre via www.ccdc.cam.ac.uk/data_request/cif.

Water adsorption measurement



A water adsorption amount in sample pellets during conductivity measurement were estimated by the subtraction of initial weight (sample pellet + electrode + plastic container and PARAFILM[®] (to avoid humidity change during weighing))

from the weight after keeping at 95% RH and 25 °C in a humidity controllable incubator for more than 12 h. We did three trials and results are in the following table.

Entry	Sample amount (mg, mmol)	S (m ²)	T (m)	Adsorbed water amount V' (mg)	Total water amount in a pellet V (mg, mmol)	H ₂ O:TPHAP ⁻ (molar ratio)
1	28.7, 0.0617	1.33×10^{-4}	1.8×10^{-4}	21.8	23.2, 1.29	20.9 : 1
2	27.8, 0.0598	1.33×10^{-4}	1.8×10^{-4}	29.0	30.4, 1.69	28.2 : 1
3	58.4, 0.126	1.33×10^{-4}	3.7×10^{-4}	24.0	26.9, 1.49	11.9 : 1

Table S1. Water adsorption result using pellet sample of K⁺TPHAP⁻ crystalline powder **1**.

Determination of diffusion coefficient of water in **2** by PFG ¹H-NMR

Sample preparation for the measurement of ¹H self-diffusion coefficient (D) of **2** was performed by packing **1** (415 mg) into an NMR sample tube of 5 mm outer diameter. After addition of 509 μ L water into the sample, flame-sealed sample tube was kept 40 °C in an oven for 1 d. The control sample (**1**, 430 mg) was also flame-sealed into an NMR sample tube of 5 mm outer diameter after evacuation. ¹H self-diffusion coefficient (D) of **2** was estimated from signal reduction against the magnitude of g by the following equation $I/I_0 (= \exp[-D\gamma^2 g^2 \delta^2 (\Delta - \delta/3)])$, where I and I_0 are the signal intensities at each g and at no g , respectively, and γ is the gyromagnetic ratio.^{S6} Applied gradient strengths reached 800 G cm⁻¹ while gradient (δ) on and gradient delay (Δ) time values are 0.5 ms and 3.55 ms, respectively. The

resulting echo profile versus gradient strength is fitted to the above equation and D is extracted. The results are shown in fig. S4.

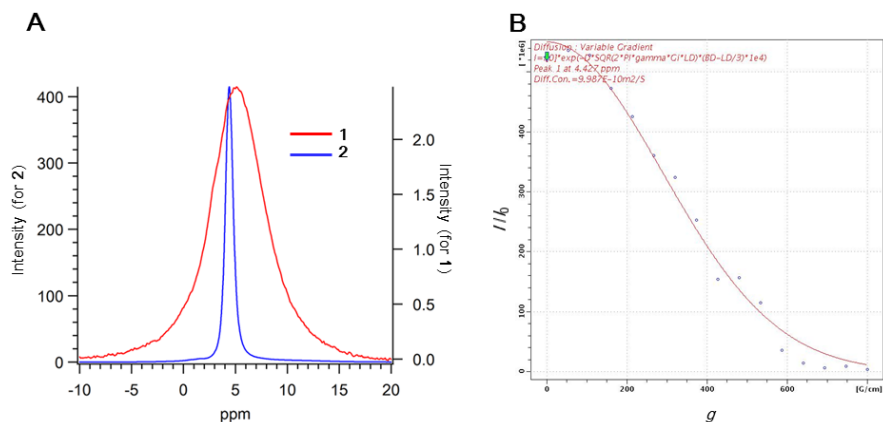


Figure S4. The results of PFG ^1H -NMR of K^+TPHAP^- crystalline powder **1** and hydrated K^+TPHAP^- powder **2**. (A) The initial solid state ^1H -NMR spectra of each sample. (B) A plot of the observed signal attenuation I/I_0 versus gradient strength g for **2**.

IR measurement of K^+TPHAP^- powders

IR spectra were recorded by the ATR method with using the corresponding powders. For the data collection of fully-hydrated powder **2**, we directly added one drop of water to single crystalline K^+TPHAP^- powder **1**.

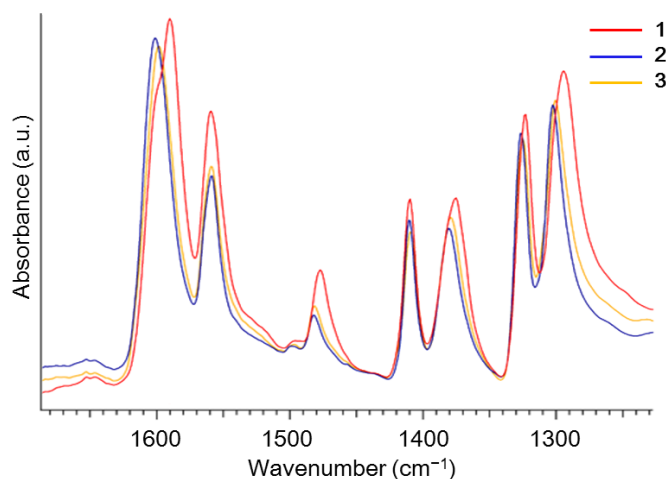


Figure S5. Blue shift of C=N and C=C stretching bands in IR spectra of K^+TPHAP^- by hydration.

Ionic conductivity measurement

The pellets for ionic conductivity measurement were prepared from ground powder **1** of K^+TPHAP^- single crystals with a mortar and a pestle. The powder **1** (35-40 mg) was put into a standard 13 mm die and pressed at 5 t for 1 minute. The pellet thickness was ~0.2 mm. The pellet shapes before and after hydration is shown in fig. S6. The XRPD pattern after hydration and drying of the pellets are shown in fig. S7.

Ionic conductivities were measured with a home-built two-electrode cell with two stainless steel blocking electrodes by a.c. impedance spectroscopy with a Solartron SI 1260 impedance/gain-phase analyzer in the frequency range 100 Hz to 0.1 MHz at various temperatures (25–80°C) and humidity (60–95% RH) after keeping the pellet under each condition for more than 12 h in a humidity controllable incubator (fig. S8). Impedance value was read at high-frequency plateau. An example is shown in fig. S9 (at 95% RH, 25°C).

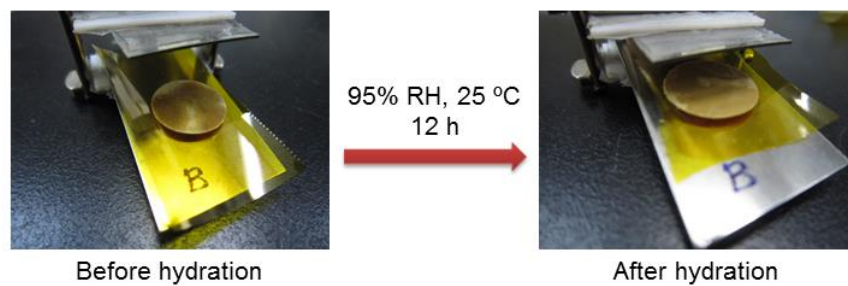


Figure S6. The pellet shapes of **1** before and after hydration.

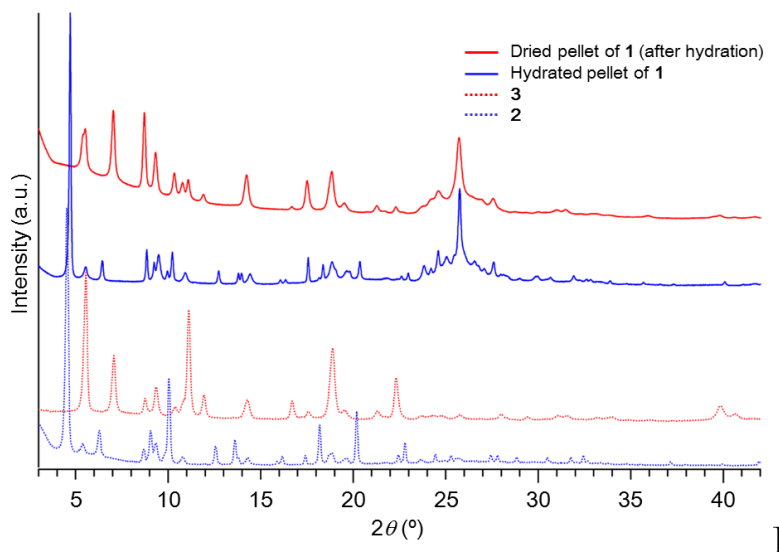
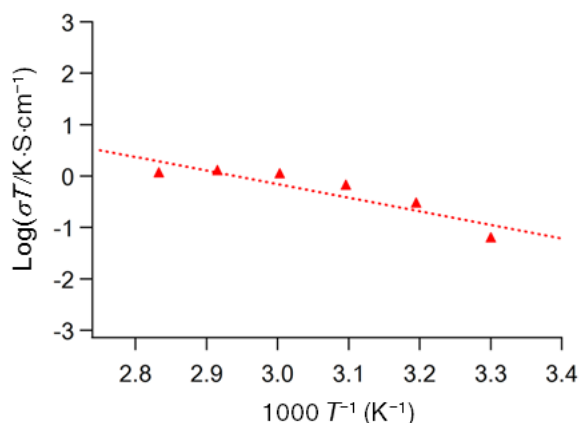


Figure S7. PXRD pattern change of pellet and non-pressed samples. Small peak shift of pellet sample data from those of non-pressed samples are coming from the small height difference. A strong and relatively broad peak at $2\theta = 26^\circ$ is attributed to preferred orientation effect.



Temperature (at 95% RH)	Adsorbed water amount
30 °C	24 mg
40 °C	25.2 mg
50 °C	26.7 mg
60 °C	22.9 mg
70 °C	11.6 mg
80 °C	3.3 mg

Figure S8. Arrhenius plot of **1** at 95% RH. The conductivity at 25 °C is $3.4 \times 10^{-3} \text{ S cm}^{-1}$ which is comparable value to those of other systems such as Li^+ conducting MOF^{S7} ($3.1 \times 10^{-4} \text{ S cm}^{-1}$ at 27 °C) and K^+ conducting polymer electrolyte (ca 0.05 S cm^{-1} at 25 °C).^{S8} The obtained activation energy E_a is 0.52 eV. This value is relatively higher than that of the proton conductor working on the Grotthuss mechanism. This result suggests that there is other process especially vehicle mechanism of K^+ contributing to ion conduction in present system. However, it is difficult to make a clear conclusion since the glass transition temperature of our sample which is required for model fitting under humid conditions is hard to obtain. In addition, the data could not be fit well by simple Arrhenius equation. This can be originated by the different water adsorption value depending on temperatures at 95% RH. Water adsorption values were measured by the subtraction of initial weight (sample pellet of **1** (58.4 mg) + electrode + plastic case and PARAFILM[®] (to avoid humidity change during weighing)) from the weight after keeping at 95% RH and various temperatures in a humidity controllable incubator for 12 h. As shown in the table, adsorbed water amount even at low temperatures (30 °C, 40 °C) showed different values. The smaller amount of water in the sample kept at higher temperatures can be explained by the ease of water evaporation.

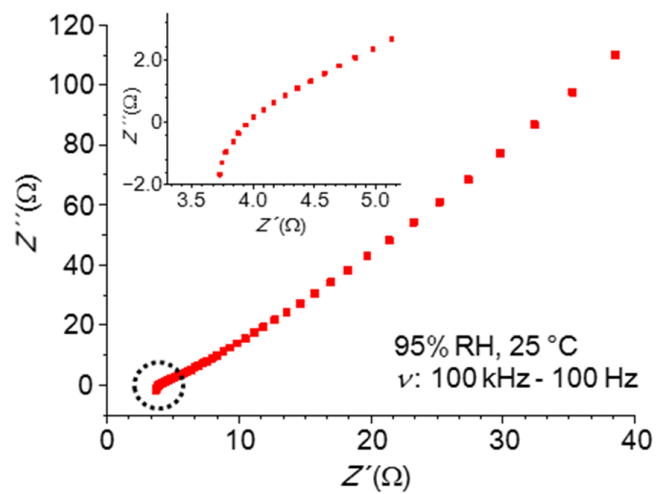


Figure S9. Nyquist plot of K^+TPHAP^- at 95%RH, 25 °C. Inset figure shows the magnified plot of the region encircled with dotted line.

References

- S1. Y. Yakiyama, A. Ueda, Y. Morita, M. Kawano, *Chem. Commun.* 2012, **48**, 10651-10653.
- S2. A. Boultif, D. Louër, *J. Appl. Crystallogr.* 1991, **24**, 987-993.
- S3. W. I. F. David, K. Shankland, N. Shankland, *Chem. Commun.* 1998, 931-932.
- S4. F. Izumi, K. Momma, *Solid State Phenom.* 2007, **130**, 15-20.
- S5. K. Momma, F. Izumi, *J. Appl. Crystallogr.* 2008, **41**, 653-658.
- S6. (a) J. E. Tanner, *J. Chem. Phys.* 1970, **52**, 2523-2526; (b) T. A. Zawodzinski, Jr., M. Neeman, L. O. Sillerud, S. Gottesfeld, *J. Phys. Chem.* 1991, **95**, 6040-6044.
- S7. B. M. Wiers, M. Foo, N. P. Balsara, J. R. Long, *J. Am. Chem. Soc.* 2011, **133**, 14522-14525.
- S8. T. Okada, H. Satou, M. Okuno, M. Yuasa, *J. Phys. Chem. B* 2002, **106**, 1267-1273.